ADVANCED MATERIALS

Supporting Information

for *Adv. Mater.,* DOI: 10.1002/adma.202102091

Electrode-Induced Self-Healed Monolayer MoS_2 for High Performance Transistors and Phototransistors

Sangyeon Pak, Seunghun Jang, Taehun Kim, Jungmoon Lim, Jae Seok Hwang, Yuljae Cho, Hyunju Chang, A-Rang Jang, Kyung-Ho Park, John Hong, and SeungNam Cha**

Supporting Information

for

Electrode-induced self-healed monolayer MoS_2 for high performance transistors and phototransistors

Sangyeon Pak, Seunghun Jang, Taehun Kim, Jungmoon Lim, Jae Seok Hwang, Yuljae Cho, Hyunju Chang, A-Rang Jang, Kyung-Ho Park, John Hong, SeungNam Cha**

Dr. S. Pak, T. Kim, J. Lim, Prof. S. Cha
Department of Physics, Sungkyunkwan University (SKKU), Suwon, Gyeonggi-do 16419, Republic of Korea
Email: chasn@skku.edu

Dr. S. Jang, Dr. H. Chang
Chemical Data-Driven Research Center, Korea Research Institute of Chemical Technology (KRICT), Gajeong-ro 141, Daejeon, 34114 Republic of Korea

J. Hwang, Dr. K.-H Park
Nanodevices Laboratory, Korea Advanced Nano Fab Center (KANC), Suwon 16229, Republic of Korea

Prof. Y. Cho
University of Michigan, Shanghai Jiao Tong University Joint Institute, Shanghai Jiao Tong University, Minhang District, Shanghai 200240, P.R. China

Prof. A.-R. Jang
Department of Electrical Engineering, Semyung University, Chungcheongbuk-do 27136, Republic of Korea

Prof. J. Hong
School of Materials Science and Engineering, Kookmin University, Seoul, 02707, Republic of Korea
Email: johnhong@kookmin.ac.kr

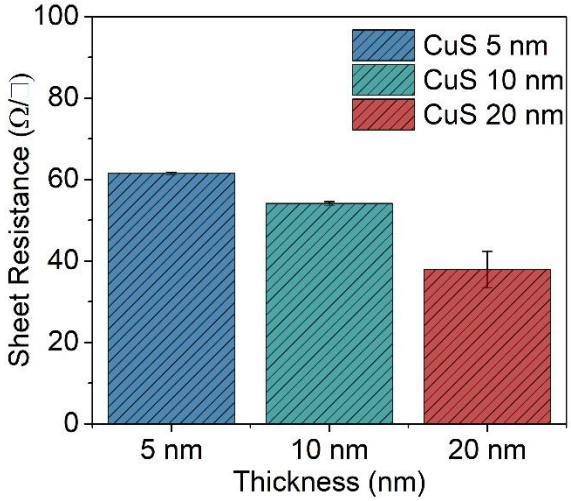

Figure S1. Sheet resistance of CuS electrode with different thickness.

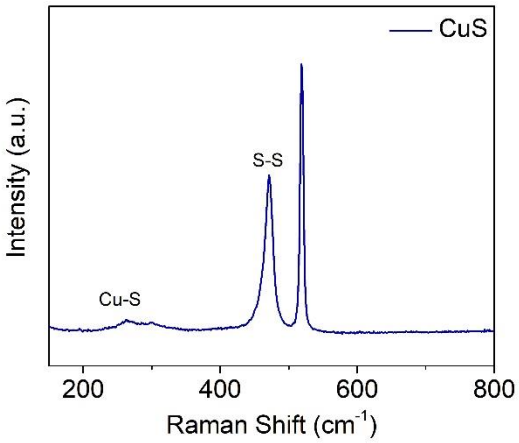

Figure S2. Raman spectrum of CuS film. Cu-S vibration and S-S vibration peaks were found at 263 cm^{-1} and 471 cm^{-1}, respectively.

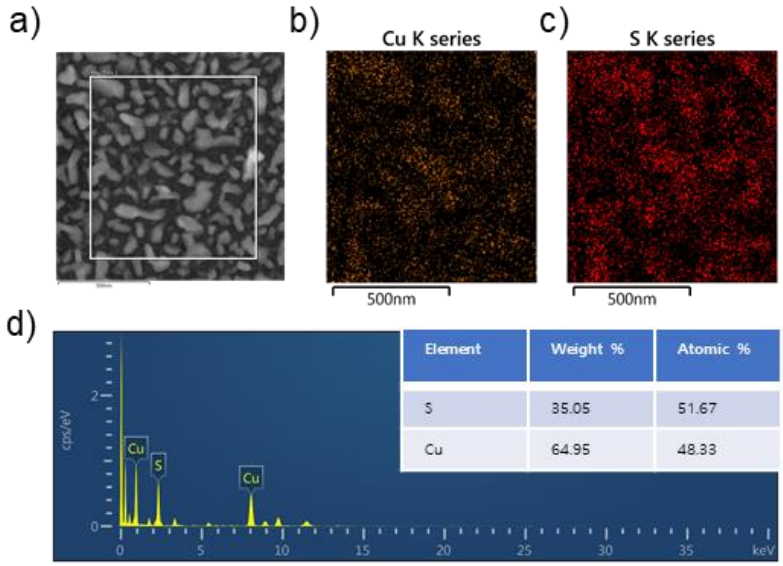

Figure S3. TEM-EDS a-c) mapping image and d) spectrum of CuS.

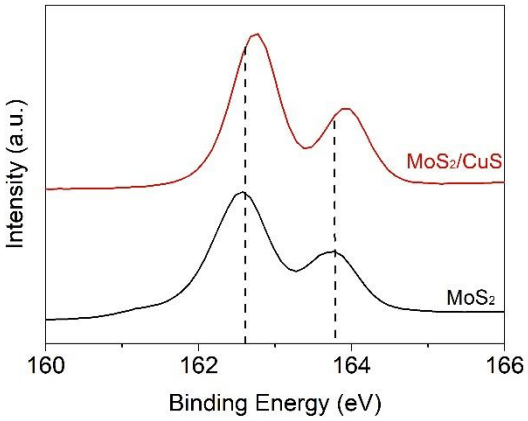

Figure S4. X-ray photoelectron spectroscopy characterization of S 2p state of MoS_2 and MoS_2/CuS.

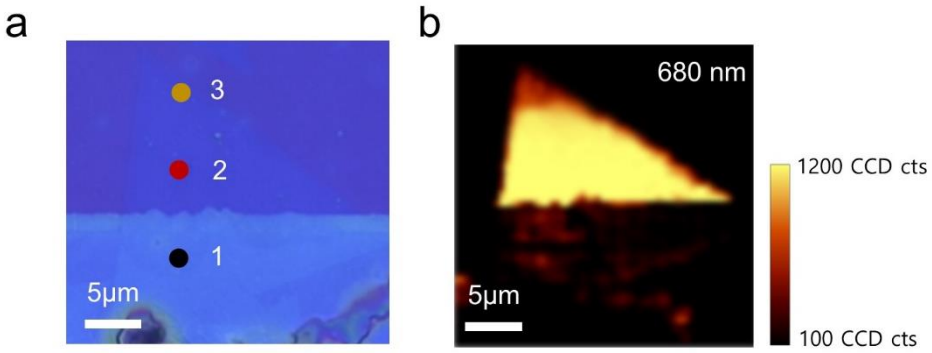

Figure S5. a) An optical microscope image of MoS_2/CuS Hybrid structure. The region 1 is the MoS_2/CuS overlapped region, while the region 2 and 3 are MoS_2 only. b) PL mapping image taken from a.

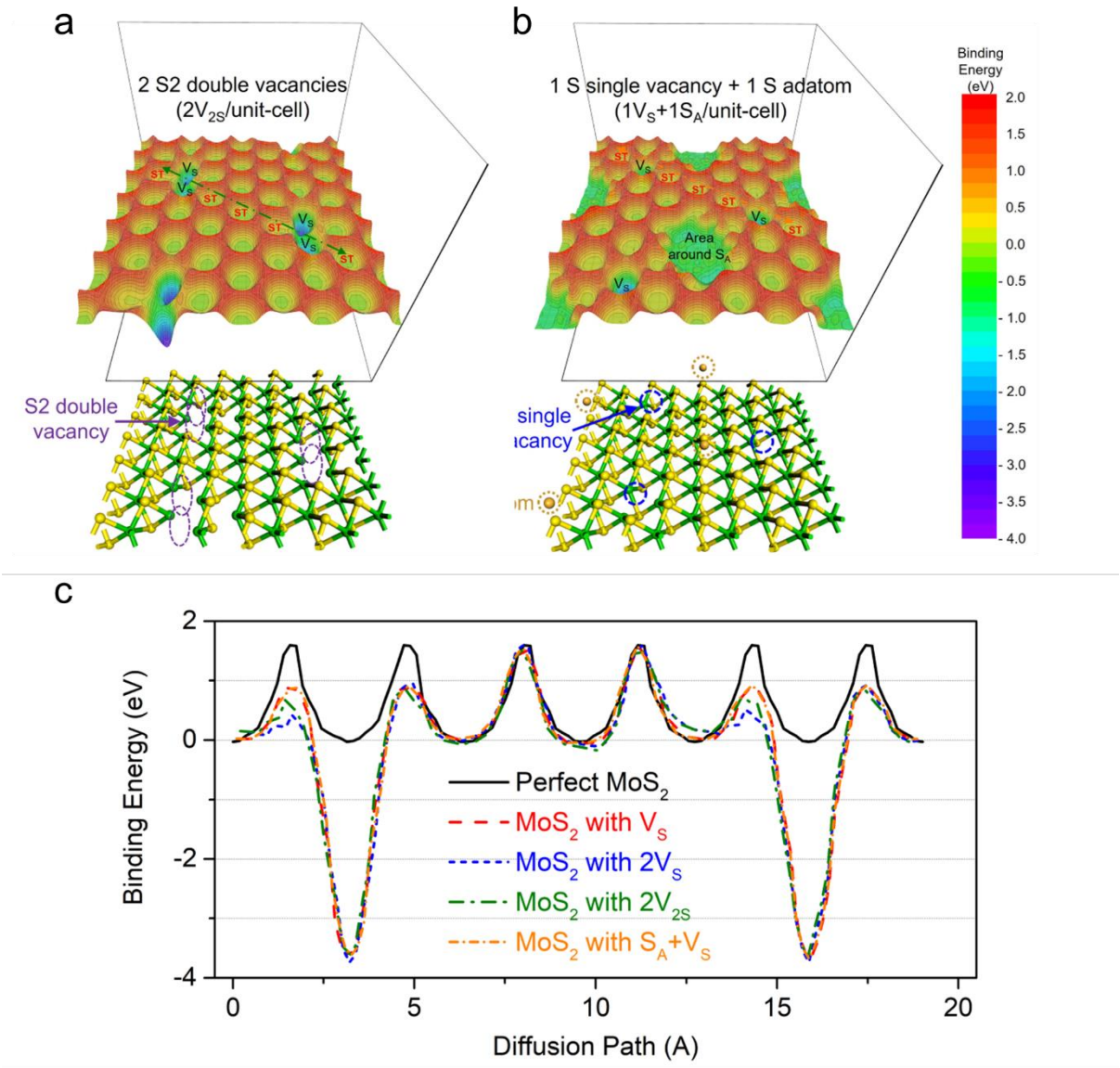

Figure S6**.** BESs of a sulfur adatom placed in different positions (upper) and optimized atomic surface structures (lower) on a) MoS_2 with two S2 double vacancies, b) MoS_2 with sulfur single vacancy and adatom. The yellow and green spheres represent sulfur and molybdenum atoms, respectively. c) Energy barrier profiles for proposed surface diffusion paths (double-headed arrows in a,b and other proposed paths shown in Figure 3) of a sulfur adatom.

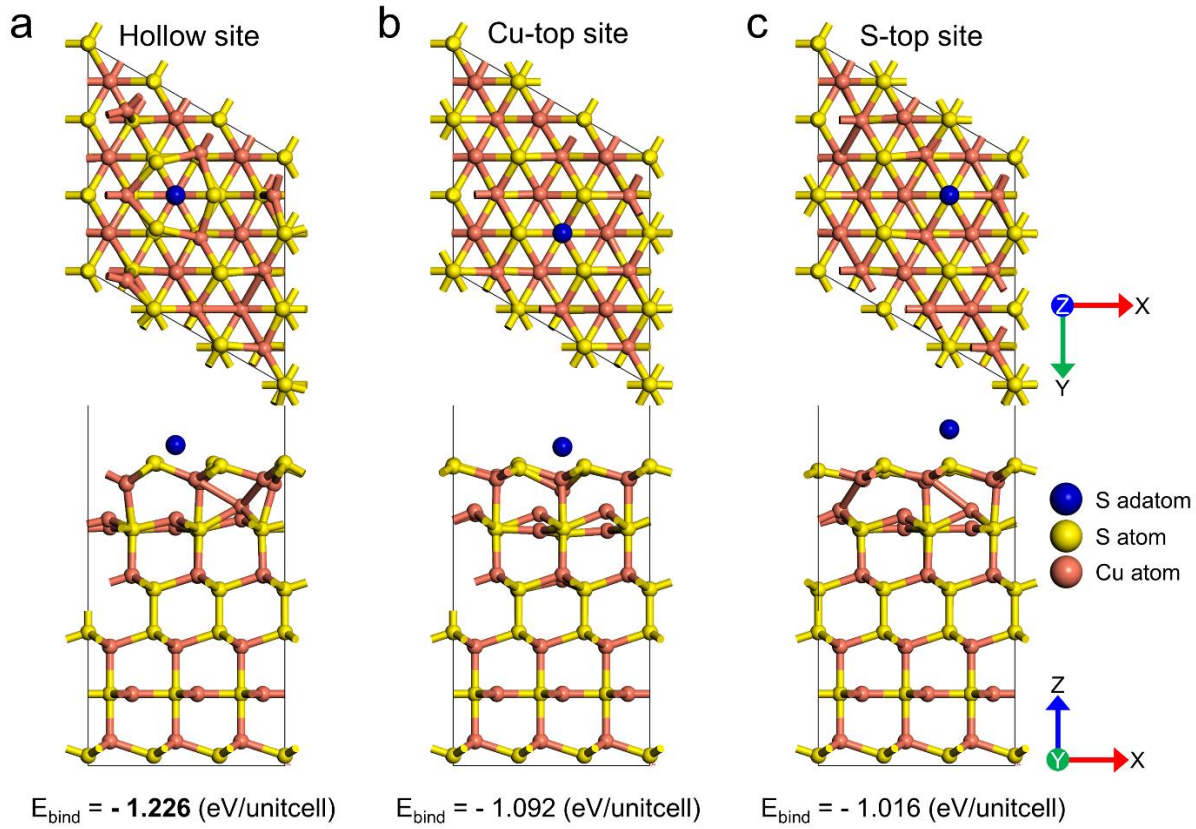

Figure S7. Top (upper) and side (lower) views of the optimized atomic structures of the S adatom adsorbed on hollow (a), Cu-top (b), and S-top (c) sites of pristine CuS surface. The blue, yellow, and green spheres represent sulfur adatom, sulfur atom and copper atom, respectively. The binding energy was defined as $E_{bind} = E_{S\text{-}adatom/CuS\text{-}Surface} - (E_{S\text{-}adatom} + E_{CuS\text{-}Surface})$, where $E_{S\text{-}adatom/CuS\text{-}Surface}$ is the total energy of the total system that the S adatom is adsorbed on the pristine CuS surface, and $E_{S\text{-}adatom}$ and $E_{CuS\text{-}Surface}$ are the total energies of the isolated S atom and the pristine CuS surface, respectively.

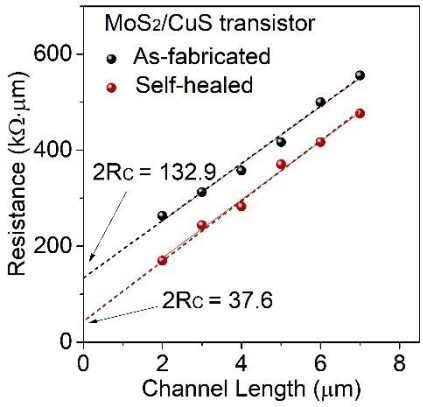

Figure S8. Contact resistance of the as-fabricated and self-healed device. The total two-probe resistance of MoS_2 channels were measured with varying channel length. The total resistance $R = 2R_C + R_{sh}\frac{L}{W}$, where R_C is the contact resistance, R_{sh} is the channel resistance. The R_C value was estimated by extrapolating to zero channel length, which was found to be 66.5 KΩ·μm and 18.8 KΩ·μm for the as-fabricated and self-healed device, respectively.

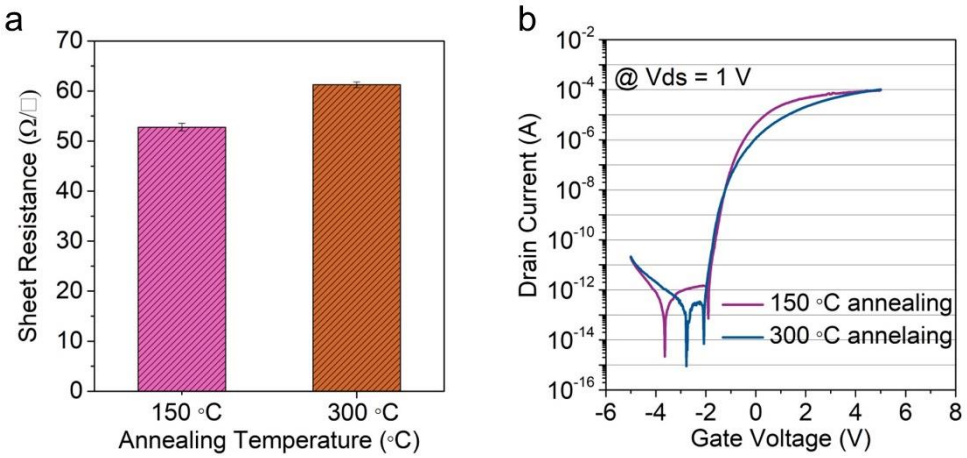

Figure S9. a) Sheet resistance of the CuS electrode and b) transfer curve of the MoS_2/CuS after post annealing temperature of 150 ˚C and 300 ˚C.

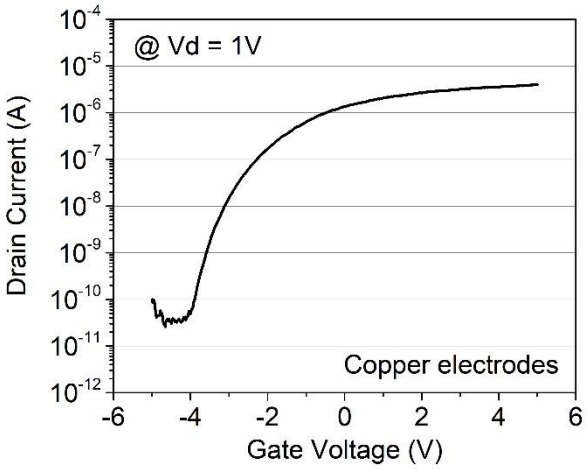

Figure S10. Transfer curve measured for MoS_2 transistor with Cu electrode. The device shows On/Off ratio of 10^6 and field effect mobility of 3.7-9 $cm^2V^{-1}s^{-1}$, which are orders of magnitude smaller than the values obtained for MoS_2/CuS devices. The device shows no observable SVSH effect after the mild thermal annealing.

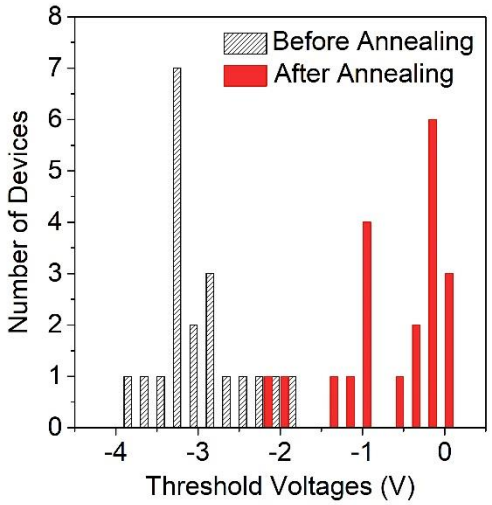

Figure S11. Statistical chart showing the threshold voltages of MoS_2/CuS transistor before and after the thermal annealing.

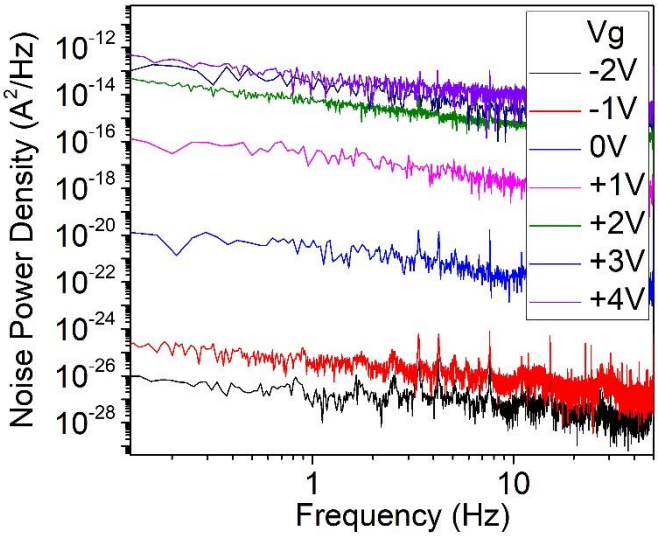

Figure S12. Noise power density of dark current with varying gate voltages.

The detectivity, *D**, at 1 Hz bandwidth is defined as $D^* = \frac{\sqrt{AB}}{NEP}$ in unit of jones (1 jones = 1 $cmHz^{1/2}W^{-1}$), where *A* is the device active area and *B* is the noise bandwidth, and *NEP* is the noise equivalent power ($NEP = i_n/R$) assuming that the shot noise, $i_n = (2eI_{dark})^{\frac{1}{2}}$, from the dark current is the major contributor to the noise. As shown in Figure 5a, dark current level is significantly low (in the range of sub-picoamphere) in the self-healed devices, which merit such high value of the maximum detectivity. Such low dark current level leads to considerable decrease in the spectral noise density shown in Figure S12. Dark current noise in the phototransistors was measured using a Stanford Research SR830 lock-in amplifier as measured elsewhere.[1-3] Also, the measurement was carried out in an electrically and optically shielded probe station which is placed on a floating table to minimize vibrational noise. NEP is then calculated using the noise power density at 1 Hz, and R is calculated from Figure 5a. Then, the D* is calculated based on the NEP and the device active area.

Ref	Configuration	Method	Mobility @ RT ($cm^2V^{-1}s^{-1}$)	On/Off Ratio	SS (mV/dec)	Notes
[4]	Top-gated	Exfoliation	217	10^8	74	
[5]	Top-gated	Exfoliation	320	10^6		
[6]	Top-gated	Exfoliation	1090	10^8	178	
[7]	Top-gated	CVD	55	10^7		
[8]	Back-gated	Exfoliation	70			Graphene contact
[9]	Back-gated	Exfoliation	10	10^6		
[10]	Back-gated	Exfoliation	260	10^6		Metal transfer
[11]	Back-gated	Exfoliation	167	10^6		In Contact
[12]	Back-gated	Exfoliation	50	10^7	100	Phase engineering
[13]	Back-gated	CVD	8	10^7		
[14]	Back-gated	CVD	0.04			
[15]	Back-gated	CVD	5.4	10^5		
[16]	Back-gated	CVD	24	10^9		
[17]	Back-gated	CVD	10	10^8		
[18]	Back-gated	CVD	1.8	10^4		Inkjet printed contact
[19]	Back-gated Top-gated	CVD	0.7 32.3	10^3		
This Work	**Back-gated**	**CVD**	**100**	**10^8**	**120**	**CuS contact**

Table S1. Performance comparison of field effect transistors based on monolayered MoS_2.

Ref	Device Configuration	Vacancy-Healing Method	Device Electrical Properties
[20] Nature Communications, 2017	Back-gated CVD-MoS_2	poly(4-styrenesulfonate) (PSS)	Mobility ~ 0.26 $cm^2V^{-1}s^{-1}$ Photoresponsivity ~ 5.12 A/W
[21] Science, 2015	Back-gated Exfoliated MoS_2	bis(trifluoromethane)sulfonimide (TFSI)	On/Off Ratio ~ 10^5
[22]ACS Nano, 2015	Back-gated Exfoliated MoS_2	Alkanethiol	Mobility ~ 0.32~35.37 $cm^2V^{-1}s^{-1}$
[23]Journal of Applied Physics, 2016	Back-gated Exfoliated MoS_2	$(NH_4)S$	SS ~ 2.5 V/dec
[24]ACS Nano, 2015	Back-gated Exfoliated MoS_2	mercaptoethylamine (MEA), 1H,1H,2H,2H-perfluorodecanethiol (FDT)	$\Delta n = 7 \times 10^{11}$ cm^{-2}
This Work	**Back-gated CVD-MoS_2**	**CuS contact**	**Mobility ~ 100 $cm^2V^{-1}s^{-1}$ On/Off Ratio > 10^8 SS < 120 mV/dec**

Table S2. Performance comparison of transistors based on vacancy-healed 2D MoS_2.

Ref	Pristine MoS_2-based Phototransistors	Laser (nm)	Photoresponsivity (A/W)	Detectivity (Jones)	Response Time
[25]	CVD 1L-MoS_2	532	2200	-	-
[26]	CVD 1L-MoS_2	450	178	-	>30 s
This Work	**CVD 1L-MoS_2**	**450**	**$>10^4$**	**$>10^{13}$**	**90-160 ms**
[3]	Exf 1L-MoS_2	561	880	-	4-9 s
[27]	Exf ML-MoS_2	400-700	10^4	-	-
[28]	Exf ML-MoS_2	630	120×10^{-3}	$<10^{11}$	
[29]	Exf ML-MoS_2	637	96.8	$>10^{14}$	0.4-200 ms
[2]	Exf ML-MoS_2	635	10^4	$<10^{12}$	0.01-10 s

Table S3. Performance comparison of phototransistors based on 2D MoS_2.

References

[1] G. Konstantatos, J. Clifford, L. Levina, E. H. Sargent, *Nat. Photonics* **2007**, 1, 531.
[2] D. Kufer, G. Konstantatos, *Nano Lett.* **2015**, 15, 7307.
[3] O. Lopez-Sanchez, D. Lembke, M. Kayci, A. Radenovic, A. Kis, *Nat. Nanotechnol.* **2013**, 8, 497.
[4] B. Radisavljevic, A. Radenovic, J. Brivio, V. Giacometti, A. Kis, *Nat. Nanotechnol.* **2011**, 6, 147.
[5] B. Radisavljevic, M. Whitwick, A. Kis, *ACS Nano*, 5, 9934.
[6] D. Lembke, A. Kis, *ACS Nano*, 6, 10070.
[7] A. Sanne, R. Ghosh, A. Rai, H. C. P. Movva, A. Sharma, R. Rao, L. Mathew, S. K. Banerjee, *Appl. Phys. Lett.* **2015**, 106, 062101.
[8] Y. Liu, H. Wu, H. C. Cheng, S. Yang, E. B. Zhu, Q. Y. He, M. N. Ding, D. H. Li, J. Guo, N. O. Weiss, Y. Huang, X. F. Duan, *Nano Lett.* **2015**, 15, 3030.
[9] D. J. Late, B. Liu, H. S. Matte, V. P. Dravid, C. N. Rao, *ACS Nano* **2012**, 6, 5635.
[10] Y. Liu, J. Guo, E. B. Zhu, L. Liao, S. J. Lee, M. N. Ding, I. Shakir, V. Gambin, Y. Huang, X. F. Duan, *Nature* **2018**, 557, 696.
[11] Y. Wang, J. C. Kim, R. J. Wu, J. Martinez, X. J. Song, J. Yang, F. Zhao, K. A. Mkhoyan, H. Y. Jeong, M. Chhowalla, *Nature* **2019**, 568, 70.
[12] R. Kappera, D. Voiry, S. Yalcin, B. Branch, G. Gupta, A. Mohite, M. Chhowalla, *Nat. Mater.* **2014**, 13, 1128.
[13] A. M. van der Zande, P. Y. Huang, D. A. Chenet, T. C. Berkelbach, Y. You, G. H. Lee, T. F. Heinz, D. R. Reichman, D. A. Muller, J. C. Hone, *Nat. Mater.* **2013**, 12, 554.
[14] Y. J. Zhan, Z. Liu, S. Najmaei, P. M. Ajayan, J. Lou, *Small* **2012**, 8, 966.
[15] W. Park, J. Baik, T. Y. Kim, K. Cho, W. K. Hong, H. J. Shin, T. Lee, *ACS Nano* **2014**, 8, 4961.
[16] Z. F. Zhang, X. L. Xu, J. Song, Q. G. Gao, S. C. Li, Q. L. Hu, X. F. Li, Y. Q. Wu, *Appl. Phys. Lett.* **2018**, 113, 202103.
[17] H. Kwon, S. Garg, J. H. Park, Y. Jeong, S. Yu, S. M. Kim, P. Kung, S. Im, *Npj 2d Mater Appl* **2019**, 3, 9.
[18] T. Y. Kim, M. Amani, G. H. Ahn, Y. Song, A. Javey, S. Chung, T. Lee, *ACS Nano* **2016**, 10, 2819.
[19] H. Kim, W. Kim, M. O'Brien, N. McEvoy, C. Yim, M. Marcia, F. Hauke, A. Hirsch, G. T. Kim, G. S. Duesberg, *Nanoscale* **2018**, 10, 17557.
[20] X. K. Zhang, Q. L. Liao, S. Liu, Z. Kang, Z. Zhang, J. L. Du, F. Li, S. H. Zhang, J. K. Xiao, B. S. Liu, Y. Ou, X. Z. Liu, L. Gu, Y. Zhang, *Nat. Commun.* **2017**, 8, 15881.
[21] M. Amani, D.-H. Lien, D. Kiriya, J. Xiao, A. Azcatl, J. Noh, S. R. Madhvapathy, R. Addou, K. C. Santosh, M. Dubey, K. Cho, R. M. Wallace, S.-C. Lee, J.-H. He, J. W. Ager, X. Zhang, E. Yablonovitch, A. Javey, *Science* **2015**, 350, 1065.
[22] K. Cho, M. Min, T.-Y. Y. Kim, H. Jeong, J. Pak, J.-K. K. Kim, J. Jang, S. J. Yun, Y. H. Lee, W.-K. K. Hong, T. Lee, *ACS Nano* **2015**, 9, 8044.
[23] Y. Wang, L. Qi, L. Shen, Y. H. Wu, *J. Appl. Phys.* **2016**, 119, 154301.
[24] D. M. Sim, M. Kim, S. Yim, M. J. Choi, J. Choi, S. Yoo, Y. S. Jung, *ACS Nano* **2015**, 9, 12115.
[25] W. Zhang, J.-K. Huang, C.-H. Chen, Y.-H. Chang, Y.-J. Cheng, L.-J. Li, *Adv. Mater.* **2013**, 25, 3456.
[26] J. Lee, S. Pak, Y.-W. Lee, Y. Cho, J. Hong, P. Giraud, H. S. Shin, S. M. Morris, J. I. Sohn, S. Cha, J. M. Kim, *Nat. Commun.* **2017**, 8, 14734.
[27] Y. T. Lee, J. H. Kang, K. Kwak, J. Ahn, H. T. Choi, B. K. Ju, S. H. Shokouh, S. Im, M. C. Park, D. K. Hwang, *Acs Photonics* **2018**, 5, 4745.
[28] W. Choi, M. Y. Cho, A. Konar, J. H. Lee, G. B. Cha, S. C. Hong, S. Kim, J. Kim, D. Jena, J. Joo, S. Kim, *Adv. Mater.* **2012**, 24, 5832.
[29] L. Q. Tu, R. R. Cao, X. D. Wang, Y. Chen, S. Q. Wu, F. Wang, Z. Wang, H. Shen, T. Lin, P. Zhou, X. J. Meng, W. D. Hu, Q. Liu, J. L. Wang, M. Liu, J. H. Chu, *Nat. Commun.* **2020**, 11, 101.